Amino Acids (2010) 39:1013–1021
DOI 10.1007/s00726-010-0562-y

ORIGINAL ARTICLE

Comparative metabolomics charts the impact of genotype-dependent methionine accumulation in *Arabidopsis thaliana*

Miyako Kusano · Atsushi Fukushima · Henning Redestig · Makoto Kobayashi · Hitomi Otsuki · Hitoshi Onouchi · Satoshi Naito · Masami Yokota Hirai · Kazuki Saito

Received: 18 December 2009 / Accepted: 9 March 2010 / Published online: 31 March 2010

Abstract Methionine (Met) is an essential amino acid for all organisms. In plants, Met also functions as a precursor of plant hormones, polyamines, and defense metabolites. The regulatory mechanism of Met biosynthesis is highly complex and, despite its great importance, remains unclear. To investigate how accumulation of Met influences metabolism as a whole in *Arabidopsis*, three *methionine over-accumulation* (*mto*) mutants were examined using a gas chromatography–mass spectrometry-based metabolomics approach. Multivariate statistical analyses of the three *mto* mutants (*mto1*, *mto2*, and *mto3*) revealed distinct metabolomic phenotypes. Orthogonal projection to latent structures–discriminant analysis highlighted discriminative metabolites contributing to the separation of each mutant and the corresponding control samples. Though Met accumulation in *mto1* had no dramatic effect on other metabolic pathways except for the aspartate family, metabolite profiles of *mto2* and *mto*3 indicated that several extensive pathways were affected in addition to over-accumulation of Met. The pronounced changes in metabolic pathways in both *mto2* and *mto3* were associated with polyamines. The findings suggest that our metabolomics approach not only can reveal the impact of Met over-accumulation on metabolism, but also may provide clues to identify crucial pathways for regulation of metabolism in plants.

Keywords *mto* · Metabolite profiling · Polyamines · Multivariate statistical analysis

M. Kusano and A. Fukushima contributed equally to this work.

Electronic supplementary material The online version of this article (doi:10.1007/s00726-010-0562-y) contains supplementary material, which is available to authorized users.

M. Kusano · A. Fukushima · H. Redestig · M. Kobayashi · H. Otsuki · M. Y. Hirai (✉) · K. Saito
RIKEN Plant Science Center, Yokohama, Kanagawa 230-0045, Japan
e-mail: myhirai@psc.riken.jp

M. Kusano · A. Fukushima · H. Onouchi · M. Y. Hirai
JST, CREST, 4-1-8 Hon-chou, Kawaguchi, Saitama 332-0012, Japan

H. Onouchi · S. Naito
Division of Applied Bioscience, Graduate School of Agriculture, Hokkaido University, Sapporo 060-8589, Japan

S. Naito
Division of Life Science, Graduate School of Life Science, Hokkaido University, Sapporo 060-8589, Japan

K. Saito (✉)
Graduate School of Pharmaceutical Sciences, Chiba University, Chiba 263-8522, Japan
e-mail: ksaito@faculty.chiba-u.jp

Introduction

Methionine (Met) is an essential amino acid in all organisms. In plants, Met is catabolized as an important precursor for production of a variety of important metabolites, including the plant hormone ethylene, polyamines, and one of the groups of defense compounds, glucosinolates (Hesse and Hoefgen 2003). Met belongs to the aspartate (Asp) family, and the biosynthesis of Met is strictly regulated in higher plants (Azevedo et al. 2006).

To elucidate how Met levels are maintained through synthesis from the Asp family, three mutant *methionine over-accumulation* (*mto*) loci (*mto1*, *mto2*, and *mto3*) have been isolated in the model plant, *Arabidopsis thaliana* (Goto et al. 2005). Each mutation disrupts different

processes in the metabolic pathway (Fig. 1a), causing over-accumulation of Met content. The *mto1* plants have a single functional mutation in the first exon of the gene encoding cystathionine γ-synthase (CGS) (Inaba et al. 1994; Chiba et al. 1999; Suzuki et al. 2001; Onouchi et al. 2005), which catalyzes the first committed step of the Met biosynthetic pathway. The mutation in *mto1* disrupts the negative feedback regulation of the pathway, thereby causing a 40-fold increase in the Met level. The *mto2* mutant carries a mutation within the gene encoding threonine synthase (TS), which catalyzes a reaction at the branch point between Met and threonine (Thr) biosyntheses (Bartlem et al. 2000). Because of reduced competition for the common *O*-phosphohomoserine (OPH) substrate, Met accumulation in young *mto2* rosettes was 20-fold higher than that of wild-type (WT) plants. The *mto3* plant contains a mutation in the gene encoding *S*-adenosyl-methionine synthetase 3 (SAMS3), resulting in dramatic accumulation of Met, over 200-fold that of the WT level, in young rosettes (Shen et al. 2002).

Metabolomics is a useful tool for obtaining insights into the complex regulation of metabolism in plants (Oksman-Caldentey and Saito 2005; Hall 2006; Fukushima et al. 2009b). Recently, unbiased metabolite profiling using mass spectrometry (MS) and nuclear magnetic resonance (NMR) has been applied as a multipurpose tool, for example, for genotype comparisons (Weckwerth et al. 2004; Kusano et al. 2007), characterization of unknown gene functions (Hirai et al. 2007; Yonekura-Sakakibara et al. 2008; Fukushima et al. 2009a; Okazaki et al. 2009), and evaluation of genetically modified plants (Le Gall et al. 2003; Catchpole et al. 2005; Levandi et al. 2008). Gas chromatography connected with MS (GC–MS) has been used for plant metabolite profiling since the 1980s. In particular, GC–time-of-flight/MS (GC–TOF/MS)-based metabolite profiling can detect several hundred metabolites for each sample, including amino acids, organic acids, sugars, and sugar alcohols. Using GC–TOF/MS, we have previously characterized the genotype-dependent metabolomic phenotype (metabotype) of *mto1* and *tt4* (lacking the chalcone synthase gene involved in flavonoid biosynthesis) mutants (Kusano et al. 2007). Remarkable increases in metabolite levels, including Met and *S*-adenosyl-methionine (SAM), were observed in *mto1* together with other metabolite changes.

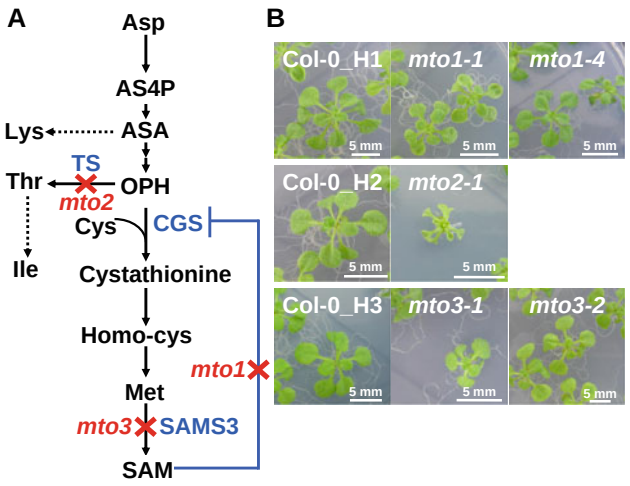

Fig. 1 An overview of the respective mutation in the aspartate-family biosynthetic pathway in each *Arabidopsis mto* mutant (**a**) and visible phenotypes of the *mto* mutants (**b**). Three mutant *mto* loci have been identified to date. Each mutation disrupts different processes within the pathway. *mto2-1* showed dwarf phenotypes (18-day-old plants). *AS4P* aspartyl-4-phosphate, *ASA* aspartate-semialdehyde, *OPH O*-phosphohomoserine, *Homo-cys* homocysteine, *SAM S*-adenosyl-methionine, *SAMS3 S*-adenosyl-methionine synthetase 3, *CGS* cystathionine γ-synthase, *TS* threonine synthase, *Asp* aspartate, *Cys* syteine, *Ile* isoleucine, *Lys* lysine, *Met* methionine, *Thr* threonine

To investigate the extent that Met accumulation influences metabolism in different mutants of *Arabidopsis*, we used the three *mto* mutants, *mto1*, *mto2*, and *mto3* in this study. These mutants, including five alleles *mto1-1* and *mto1-4* for *mto1*, *mto2-1* for *mto2*, *mto3-1* and *mto3-2* for *mto3*, have served as a biological model system in the elucidation of the regulatory mechanism of amino acid biosynthesis and other primary metabolic processes associated with over-accumulation of Met. We profiled metabolite abundances in each of the mutants and compared them with their WT counterparts. Each mutant plant showed distinct and specific metabolite profiles, although these mutants all over-accumulate Met. In particular, *mto2*, which produces visibly dwarf phenotypes, exhibited the most pronounced changes in metabolite profiles including not only the Asp family, but also the glutamate (Glu) family and polyamine biosynthetic pathway. This finding suggests that TS has a critical role in normal growth by maintaining appropriate levels of Met and metabolites belonging to the Asp, Glu, and polyamine pathways in *Arabidopsis*.

Materials and methods

Plant material and harvest

The *Arabidopsis mto* mutants, *mto1-1* (in ecotype Columbia), *mto1-4* (in Columbia), *mto2* [in ecotype Wassilewskija (WS)], *mto3-1* (in WS), and *mto3-2* (in Columbia), have been described previously (Goto et al. 2005). Seedlings were grown on Murashige and Skoog medium (Wako, Osaka, Japan, #392-00591) with 0.8% agar, 1% sucrose at pH 5.8 under 16 h light/8 h dark cycles at 22°C for 18 days. Aerial parts were harvested from 4 to 10 biological replicates of each line (see Supplementary Data 1), 6 h after the onset of the light phase. The *mto* mutants were backcrossed

ten times for *mto1-1* and *mto1-4*, seven times for *mto2*, four times for *mto3-1*, and seven times for *mto3-2* to the WT accession (Col-0) before phenotypic and metabolite profiling analysis. Two independent alleles (*mto1-1* and *mto1-4*) for *mto1*, one (*mto2-1*) for *mto2*, and two (*mto3-1* and *mto3-2*) for *mto3* were used in this study. To minimize effects derived from the different harvesting periods, we compared mutants and the control plants that were harvested in the same period [hereafter called Col0_H1 (*mto1*), Col0_H2 (*mto2*), and Col0_H3 (*mto3*), Supplementary Fig. 1]. For metabolite profiling, these mutants and the corresponding WT were grown under strictly controlled conditions (Kusano et al. 2007). The *mto2* plants exhibit dwarf phenotypes, whereas there are no visible phenotypic changes in the *mto1* and *mto3* mutants when compared with the WT (Fig. 1b).

Metabolite profiling

Plants may show differences in terms of metabolite profiles, so-called 'metabotypes', even when no visible phenotypic changes can be observed (Hall 2006). To achieve a broad coverage of primary metabolites, GC-TOF/MS-based metabolite profiling was used in this study. As described previously (Kusano et al. 2007), each sample was extracted, derivatized, and analyzed using GC-TOF/MS. Five milligrams fresh weight of plant tissues was used for GC-TOF/MS analysis. The derivatized extracts, equivalent to 55.6 µg fresh weight of plant material, were injected into the GC-TOF/MS instrument. All raw data were pre-processed using a MATLAB script (version 7.0.4, The MathWorks, Natick, MA) implemented by Jonsson et al. (2005, 2006) to perform baseline correction, alignment, and peak deconvolution. Metabolite identifications were performed by comparing their mass spectra and retention time indices to those generated for authentic compounds analyzed on our instrumentation as well as those in the mass spectra and retention index libraries in the Golm Metabolome Database (Kopka et al. 2005; Schauer et al. 2005). To correct the interference, or cross-contribution, between the internal standards and native metabolites because of problems such as insufficient chromatographic resolution, the data were normalized using cross-contribution compensating multiple standard normalization (CCMN) (Redestig et al. 2009).

Statistical data analysis

Multivariate statistical analyses, comprising principal component analysis (PCA) and orthogonal projections to latent structures–discriminant analysis (OPLS-DA) (Bylesjo et al. 2006; Trygg et al. 2007), were performed using SIMCA-P 12.0 software (Umetrics AB, Umea, Sweden) with $\log_{10}$ transformation and unit variance scaling. The models were used to visualize the high-dimensional data and determine the metabolomic variation between the control WT and *mto* mutants. PCA captures the main sources of variation in an unsupervised manner, whereas OPLS-DA extracts as much of the class-separating (mutant vs. WT) variation as possible. With OPLS-DA, the variance in X (the MS profiles) is decomposed into three parts: Y-predictive, Y-orthogonal and the unmodeled residual. The Y-predictive components capture the class-separating variation (mutant vs. WT) and can be used to interpret the differences between the genotypes. The Y-orthogonal variation on the other hand models variation that is strictly unrelated to genotypic differences. With this distinction, OPLS-DA provides a convenient way to inspect the genotype-related differences without confusing them with other systematic variance coming from residual analytical bias, for example. All OPLS-DA models were validated using leave-one-out cross-validation and diagnosed using the prediction error-rate defined as the number of inaccurate predictions of left-out samples divided by the total number of samples, N. Since N was fairly low, we also computed an empirical p value, p_{CV}, by randomizing the class labels 100 times and counting the number of times we obtained a lower error-rate than with the original labels.

Statistical tests were performed using the R statistical environment (http://www.r-project.org/) on the basis of $\log_{10}$-transformed data. The resulting p values were adjusted for multiple testing using the false discovery rate (FDR) procedure (Benjamini and Hochberg 1995).

To facilitate biological interpretation of the metabolite profiles in *mto* mutants, we performed metabolite set enrichment analysis (MSEA, Redestig et al. unpublished method), which is similar to gene set enrichment analysis (GSEA) (Mootha et al. 2003). The procedure of this approach was as follows: first, unification of metabolite identifiers was done using MetMask (http://metmask.sourceforge.net, Redestig et al. submitted), which is a tool for chemical identifier linking. Metabolites were then classified into 47 groups based on the classification scheme provided by the PlantCyc compound classes database version 3.0 (Zhang et al. 2005). Detected metabolites that were not mentioned by PlantCyc were classified manually. The groups of metabolites consist of metabolites that share biological function and/or biochemical pathways. Because of the rather crude grouping, we refer to the groups as "metabolite bins", analogous to the widely used MapMan gene bins (Thimm et al. 2004). Genotype differences were estimated using the t-statistics obtained when comparing mutants and the WT. For each metabolite class the t-statistic distribution was compared with those of all other metabolites using the Kolmogorov–Smirnov test. The analysis identified classes of metabolites that were particularly affected in the corresponding comparison. The p values were FDR corrected to adjust for multiple testing.

Results

Multivariate statistical analysis of metabolome data reveals distinct metabotypes of *mto* mutants

Using the established metabolite profiling (Kusano et al. 2007), we detected 214 metabolite peaks and their mass spectra. A total of 87 peaks comprising amino acids, organic acids, sugars, sugar alcohols, vitamins, and secondary metabolites were identified and annotated as known metabolites. Among these, 27 peaks were annotated with mass spectral tags (MSTs) (Kopka et al. 2005; Schauer et al. 2005), which have been consistently observed among several laboratories though not identified precisely. The PCA scatter plot (Fig. 2) showed that the samples were clustered with respect to their corresponding genotypes, suggesting that each *mto* plant has distinct metabolite profiles. Furthermore, *mto2* exhibited the most pronounced changes in metabolite profiles among the mutants examined. The distinction might reflect pleiotropic changes of metabolite profiles associated with the dwarf phenotype of *mto2* mutant plants (Fig. 1b).

Discriminative metabolites between *mto* mutants and WT plants were extracted using OPLS-DA

To identify the metabolites contributing to the separation between the mutant profiles and those of the WT (so-called 'discriminative metabolites'), OPLS-DA models for each genotype were examined (Fig. 3). The OPLS-DA score scatter plot of two *mto1* alleles and WT plants showed clear separation (Fig. 3a). The 34 discriminative metabolites predicted by the OPLS-DA loadings in the first Y-predictive component for *mto1* and WT were amino acids and organic acids including Met (Supplementary Table 1A). The model of the differences between *mto2* and WT indicated 120 discriminative metabolite peaks involving Glu-related metabolites, amino acids and sugars, polyamines, and intermediates in the tricarboxylic acid (TCA) cycle (Fig. 3b; Supplementary Table 1B). The score scatter plots from the model of the two *mto3* alleles and WT plants demonstrated that the distribution of *mto3-2* samples was close to that of the WT. In terms of Met content, *mto3-2* showed less accumulation than that of *mto3-1* (Goto and Naito 2002; Goto et al. 2002). This result suggests that the similarity of the metabotype of *mto3-2* and that of WT samples and the observed accumulation of Met in *mto3-2* were related. Similar to *mto2*, metabolites involved in polyamine biosynthesis as well as the Met-related pathway were identified among 90 discriminative metabolites in *mto3-1* mutant plants (Supplementary Table 1C).

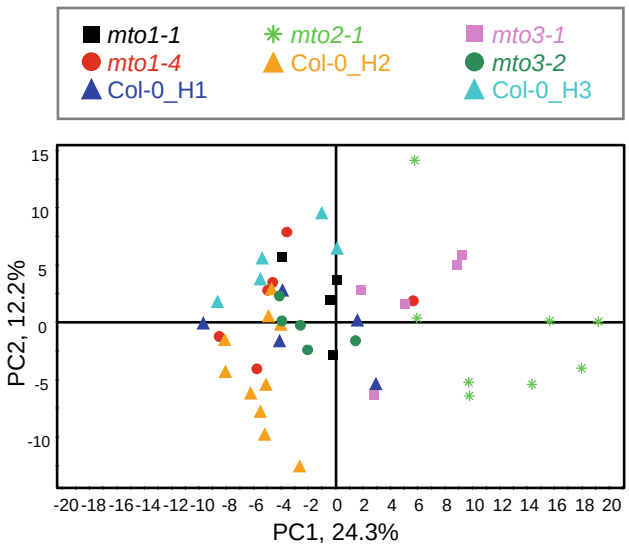

Fig. 2 Principal component analysis (PCA) of metabolomic profiles of *mto* mutants and the corresponding WT. Principal component (PC)1 and PC2 represent the first two principal components accounting for a total of 33.2% of the variance. Each plot represents an independent plant. The analysis was done using the SIMCA-P software (Umetrics AB, Umea, Sweden)

Metabolite profiling of the three *mto* mutants provides a clue to how central metabolism is affected by Met accumulation

To visualize the differences between the three *mto* plants we projected the significant metabolite changes (FDR < 0.05) between the mutants and WT on a metabolic map (Fig. 4). The changes in metabolite levels were represented as the fold-change (FC) between the mutants and WT and are listed in Supplementary Data 1. Dramatic accumulation of Met content was observed in all *mto* mutants, except for a weak allele of the *mto3* mutant, *mto3-2*. In addition, the increase in the level of methionine sulfone was over tenfold in *mto1* and *mto3*, and 20-fold in *mto2*, compared with the WT.

No obvious changes in the level of Thr in *mto2* were observed in this study, although a decrease in Thr content was reported by Bartlem et al. (2000). Furthermore, the level of upstream metabolites for Met production in the Asp family increased significantly, including the accumulation of homoserine in *mto2*. A significant increase of metabolites in the Glu and polyamine biosynthetic pathways was also observed (Fig. 4). Among metabolites belonging to the TCA cycle, the levels of malate and succinate were increased in *mto2*. These results suggest that the flux of Glu to succinate through the GABA shunt in the *mto2* mutant were intensified. The changes in the metabolite profiles of *mto3-1* overlapped partially with those of *mto2*, as exemplified by increases in the levels of Glu, ornithine, and putrescine. For other metabolites that

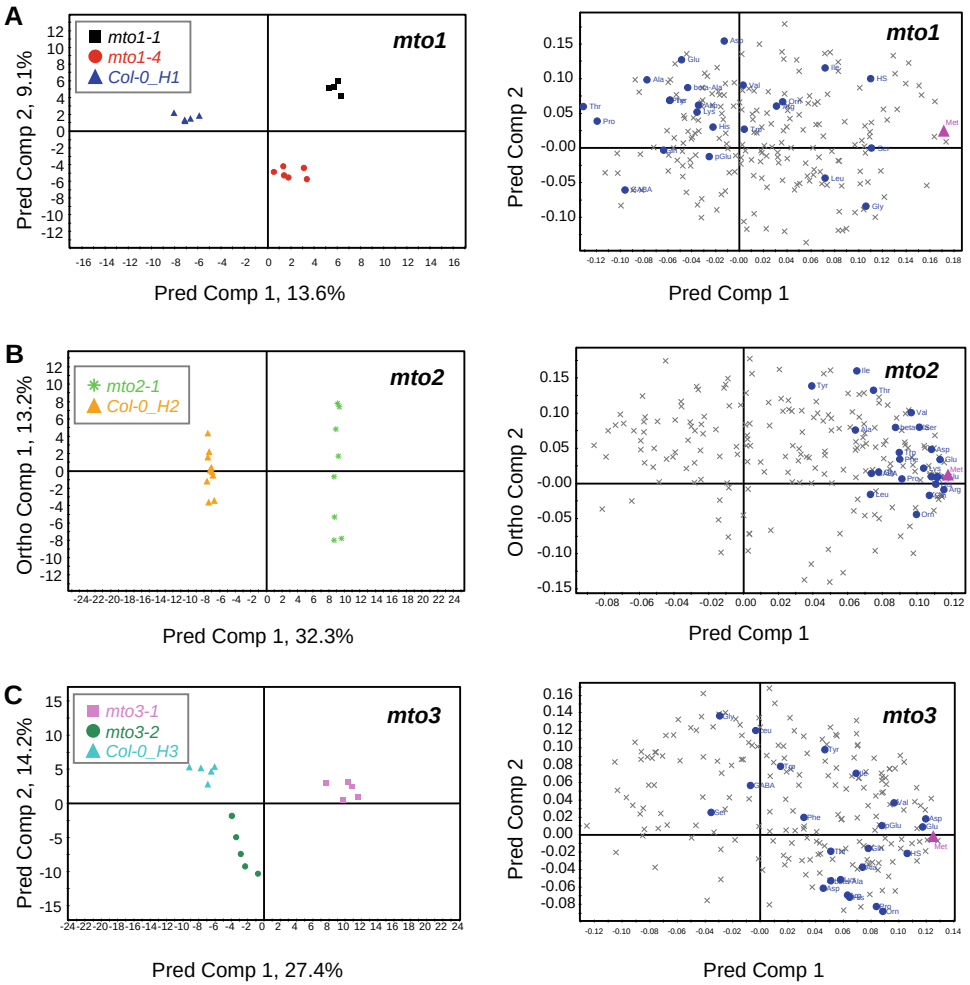

Fig. 3 OPLS-DA score scatter plot (*left*) and loading plot (*right*) of **a** *mto1*, **b** *mto2*, and **c** *mto3* samples. This analysis focused on the differences in predictive component 1 among the three models, i.e. *mto1-1*/WT, *mto2-1*/WT, and *mto3-1*/WT, according to the discriminant scores. Each point represents an independent plant in the score scatter plots and an individual metabolite in the loading plots. The *pink triangle* in each loading plot represents Met, whereas the *blue dot symbols* show amino acids except for Met. The number of each component in the score plots (except for Ortho Comp 1 in the score plot in **b** represents the sum of squares of all the x-varieties explained by the extracted components. Number of biological replicates: Col-0_H1, $n = 5$; Col-0_H2, $n = 10$; Col-0_H3, $n = 5$; *mto1-1*, $n = 4$; *mto1-4*, $n = 6$; *mto2-1*, $n = 8$; *mto3-1*, $n = 5$; *mto3-2*, $n = 5$. An associated error-rate: $2/15 = 0.13$, $p_{CV} < 0.01$ for the model in **a**; $0/18 = 0$, $p_{CV} < 0.01$ for the model in **b**; and $1/15 = 0.07$, $p_{CV} < 0.01$ for the model in **c**. *Pred Comp* predictive component, *Ortho Comp* orthogonal component, *beta-Ala* β-alanine, *GABA* γ-aminobutyrate, *Ala* alanine, *Asn* asparagine, *Arg* arginine, *Gln* glutamine, *Gly* glycine, *His* histidine, *HS* homoserine, *Leu* leucine, *Orn* ornithine, *Phe* phenylalanine, *Pro* proline, *Ser* serine, *Trp* tryptophan, *Tyr* tyrosine, and *Val* valine

were changed significantly in content in *mto3*, the levels of raffinose and dehydroascorbate were elevated in *mto3-1*, whereas the levels of intermediates in the TCA cycle, citrate (in *mto3-1* and *mto3-2*) and isocitrate (in *mto3-1*), were decreased.

To identify selectively affected metabolite bins, we performed MSEA using metabolite profiles of *mto* mutants (see "Materials and methods"). The results of MSEA suggested that there were many metabolite changes in metabolite bins in *mto2*. As shown in Supplementary Table 2, three bins, 'Synthesis (Syn)-Amines-Polyamines', 'Pyrimidines', and 'Nitrogen-Containing-Secondary-Products', showed significant changes in *mto2* compared with the corresponding WT. The levels of two bins (increased, 'Minor-Carbohydrate (CHO)-Metabolism'; and decreased, 'Central-Energy-Metabolism') changed in *mto3-1*. However, there were no significant changes in metabolite bin level in *mto1-1*, although *mto1-1* over-accumulated Met content to the same extent as the other two *mto* mutants. Taken together, these results suggest that the over-accumulation of Met mediated by the different mutations has extensive effects on metabolism, especially by mutation in *TS* and *SAMS3*.

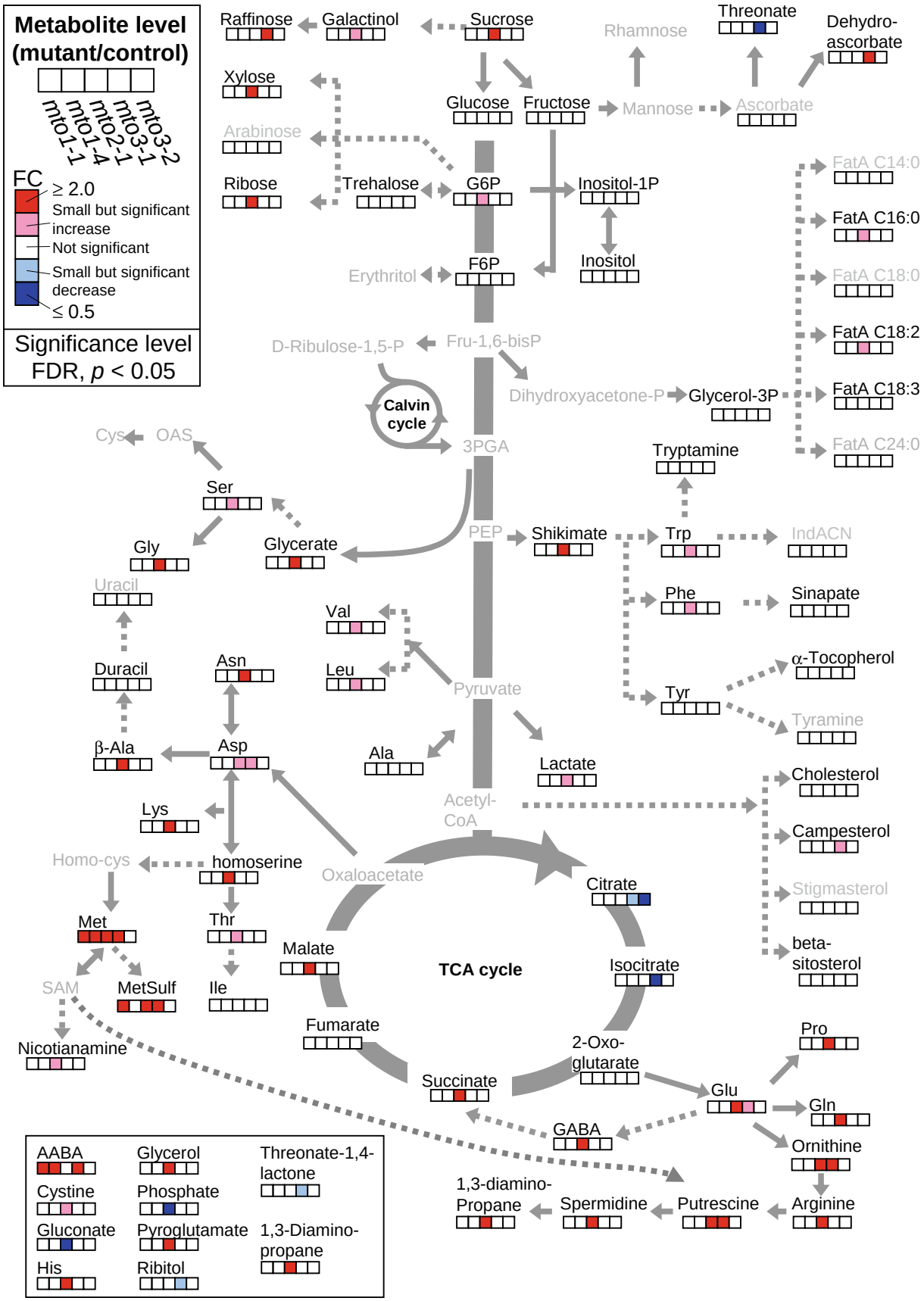
Metabolite level (mutant/control)
mto1-1
mto1-4
mto2-1
mto3-1
mto3-2
FC
≥ 2.0
Small but significant increase
Not significant
Small but significant decrease
≤ 0.5
Significance level
FDR, p < 0.05
Raffinose
Galactinol
Sucrose
Rhamnose
Threonate
Dehydro-ascorbate
Xylose
Glucose
Fructose
Mannose
Ascorbate
Arabinose
Ribose
Trehalose
G6P
Inositol-1P
Inositol
Erythritol
F6P
FatA C14:0
FatA C16:0
FatA C18:0
FatA C18:2
FatA C18:3
FatA C24:0
D-Ribulose-1,5-P
Fru-1,6-bisP
Calvin cycle
Dihydroxyacetone-P
Glycerol-3P
Cys
OAS
3PGA
Tryptamine
Ser
PEP
Shikimate
Trp
IndACN
Gly
Glycerate
Uracil
Phe
Sinapate
Val
Duracil
Asn
Leu
Pyruvate
α-Tocopherol
Tyr
Tyramine
β-Ala
Asp
Ala
Lactate
Cholesterol
Lys
Acetyl-CoA
Campesterol
Homo-cys
homoserine
Oxaloacetate
Citrate
Stigmasterol
Met
Thr
Malate
TCA cycle
Isocitrate
beta-sitosterol
SAM
MetSulf
Ile
Fumarate
Pro
Nicotianamine
2-Oxo-glutarate
Succinate
Glu
Gln
GABA
Ornithine
1,3-diamino-Propane
Spermidine
Putrescine
Arginine
AABA
Glycerol
Threonate-1,4-lactone
Cystine
Phosphate
Gluconate
Pyroglutamate
1,3-Diamino-propane
His
Ribitol

◀ **Fig. 4** Changes in metabolite profiles of *mto* mutants (*mto1-1*, *mto1-4*, *mto2-1*, *mto3-1*, and *mto3-2*; biological replicates, $n = 4$–8) compared with those of WT ($n = 5$–10). The changes were represented as the fold-change (FC) between the level of a metabolite in *mto* mutants and that in WT and are listed in Supplementary Data 1. To visualize the overall changes, significant increases or decreases are indicated in *red and blue*, respectively (FDR < 0.05). *Solid arrows* in the metabolic pathway represent a single-step reaction between two metabolites, *dashed arrows* indicate multiple steps. Metabolites in *gray characters* were not detected using the metabolite profiling. *β-Ala* β-alanine, *AABA* α-aminobutyrate, *OAS* *O*-acetyl serine, *Dihydroxyacetone-P* dihydroxyacetone-phosphate, *FatA C14:0* *n*-tetradecanoate, *FatA C16:0* *n*-hexadecanoate, *FatA C18:0* stearate, *FatA C18:2* linoleate, *FatA C18:3* linolenate, *FatA C24:0* *n*-tetracosanoate, *Fru-1,6-bisP* fructose-1,6-biphosphate, *F6P* fructose-6-phosphate, *G6P* glucose-6-phosphate, *Glycerol-3P* glycerol-3-phosphate, *IndACN* 1*H*-indole-3-acetonitrile, *Inositol-1P* inositol-1-phosphate, *MetSulf* methionine sulfone, *PEP* phosphoenolpyruvate, *3PGA* 3-phosphoglycerate, *ribulose-1,5-P* ribulose-1,5-diphosphate

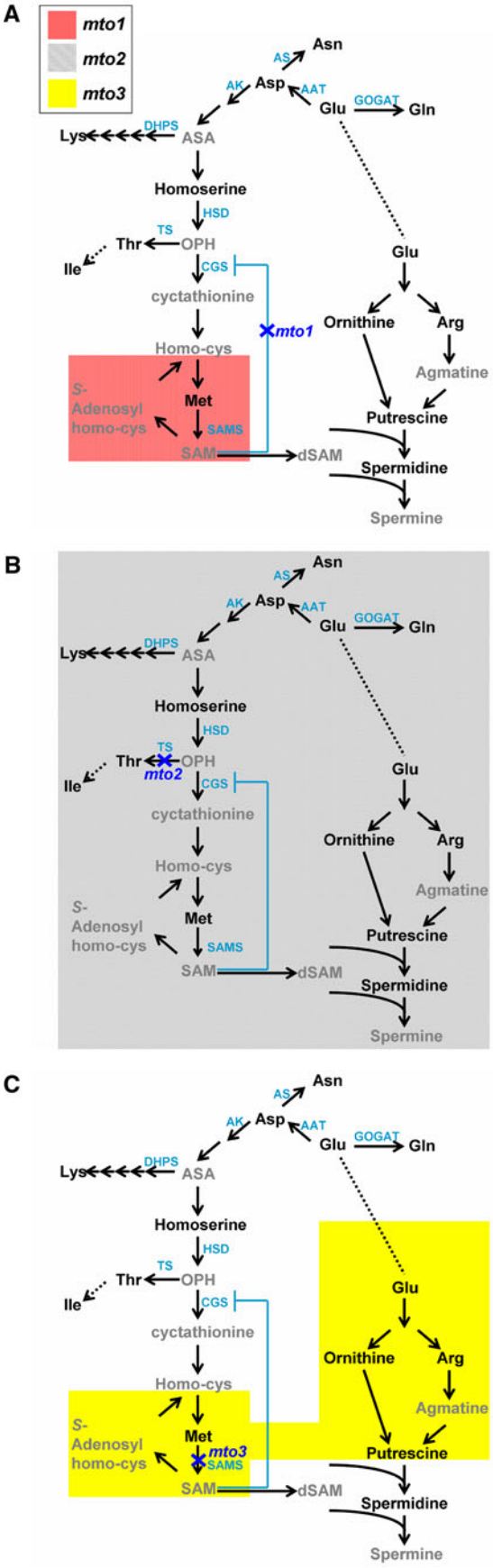

Fig. 5 Schematic overview of metabolic impacts associated with Met ▶ accumulation in *Arabidopsis*. *Thick arrows in black* indicate a single step linking two metabolites, whereas a *dashed arrow* represents multiple steps. **a** The high metabolite accumulation affected by the *mto1* mutation is highlighted with the *red box*. **b** The affected pathways in *mto2* involving biosynthesis of Asp, Glu, and polyamines are highlighted with the *gray box*. **c** The biosynthetic pathways of polyamine from Glu as well as the Met-related pathway in *mto3* plants are highlighted with the *yellow box*. *OPH* *O*-phosphohomoserine, *dSAM* decarboxylated *S*-adenosyl-methionine

Discussion

Research on the regulatory mechanism of amino acid production in the cell has a long history (Wu 2009) which has led to the identification of several enzymatic genes. For example, essential amino acids including Met, lysine, Thr, and isoleucine can be synthesized by intricate regulation in the Asp family in higher plants (Rinder et al. 2008). Met has many vital functions in plant cellular metabolism such as the production of SAM, ethylene, glucosinolate, and polyamines. To address the question of how Met accumulation influences metabolism in *Arabidopsis*, we used *mto* mutants as a model system of metabolic perturbations triggered by accumulation of Met. The advantages of our approach are as follows: first, each *mto* mutant has been relatively well-characterized in terms of the molecular mechanism. Second, we have investigated *mto1* mutant plants as a representation of our metabolomics approach. In our previous study, we found that the mutation of CGS and/or over-accumulation of Met in *mto1* also affected the metabolite-to-metabolite correlation networks (Kusano et al. 2007), suggesting that Met accumulation probably affects metabolic regulations in other pathways in *mto1*.

The multivariate statistical methods PCA and OPLS-DA were able to distinguish metabotypes (Figs. 2, 3). Met is an

important precursor of SAM, which is a common precursor for polyamine biosynthesis (Fig. 1). Subsequently, SAM is decarboxylated in a reaction catalyzed by SAM decarboxylase. The resulting dSAM is utilized as an aminopropyl donor as illustrated in Fig. 5. Our metabolomics approach using three *mto* plants clearly demonstrated that Met accumulation affects a wide range of metabolic processes from Met to metabolites in the Glu pathway and polyamine biosynthesis as well as the biosynthetic pathways associated with the TCA cycle (Fig. 4). The metabolite profiles of the three *mto* mutants showed the relationships among the origin of the mutation of each mutants, Met accumulation, and metabolite changes in the metabolic pathways (Fig. 5). The induction of Met and methionine sulfone levels was observed commonly in *mto* plants and accumulation of metabolites in the Glu and polyamine biosynthetic pathways overlapped in the *mto2* and *mto3* profiles.

The 20-fold accumulation of Met in *mto2* showed good agreement with previous results (Bartlem et al. 2000), while the metabolite profiling presented here showed no significant changes in Thr level (Fig. 4; Supplementary Data 1). Bartlem and colleagues described that prominent reduction in Thr content in *mto2* rosettes has been observed only in the young stages (until 15 day-after imbibition) of their growth (Bartlem et al. 2000). In addition, we observed accumulation of the upstream metabolites for Thr production in the Asp family. Thus, the significantly increased contents of homoserine and other metabolites belonging to the Asp family provides support that a mutation in the gene encoding TS in *mto2* plants affects processes related to Thr metabolism. Decreased TS activity or reduction in the carbon/amino skeleton flux towards Thr provides the carbon skeleton for Asp to Met production rather than Asp to Thr in *Arabidopsis* (Bartlem et al. 2000; Hesse and Hoefgen 2003). Furthermore, *mto2* displayed a dramatic increase in the metabolite bins related to polyamine and two other pathways (pyrimidine and nitrogen-containing-metabolite pathways) in addition to Met accumulation (Fig. 4; Supplementary Table 2). This suggests that Met accumulation in *mto2* enhanced other biosynthetic pathways involving polyamines. The levels of ornithine and putrescine increased in *mto3*, although intermediates in the TCA cycle showed specific accumulation patterns compared with the other *mto* mutants (Fig. 4). These results indicate that Met flux may affect accumulation of metabolites in the Glu and polyamine pathways in different manners regulated by *TS* and *SAMS3*.

Concluding remarks

The results of this study using three independent *mto* mutants indicate that Met over-accumulation affected an extensive range of pathways involved in not only Met biosynthesis, but also Glu and polyamine biosynthesis as well as metabolic pathways associated with the TCA cycle and stress-responsive metabolites in *Arabidopsis*. The metabotypes of each *mto* mutant exhibited a specific pattern. Among the *mto* mutants examined, *mto2* showed the most pronounced changes in central metabolism. The results presented here may provide a foundation for future research on the interaction of the Asp family and other metabolic pathways including the TCA cycle, GABA shunt and polyamines through Met metabolism.

Acknowledgments We thank Drs. Par Jonsson, Hans Stenlund and Thomas Moritz of UPSC, Sweden, for kindly providing the custom software for data pretreatment. The authors gratefully acknowledge the skilled technical assistance of Ms. Saeko Yasokawa and Ms. Eriko Tanaka of Hokkaido University, Sapporo, Japan. This research was supported by grants from the Japan Science and Technology Agency, CREST (project name: 'Elucidation of Amino Acid Metabolism in Plants based on Integrated Omics Analyses').

References

Azevedo RA, Lancien M, Lea PJ (2006) The aspartic acid metabolic pathway, an exciting and essential pathway in plants. Amino Acids 30:143–162

Bartlem D, Lambein I, Okamoto T, Itaya A, Uda Y, Kijima F, Tamaki Y, Nambara E, Naito S (2000) Mutation in the threonine synthase gene results in an over-accumulation of soluble methionine in Arabidopsis. Plant Physiol 123:101–110

Benjamini Y, Hochberg Y (1995) Controlling the false discovery rate: a practical and powerful approach to multiple testing. J R Stat Soc Series B 57:289–300

Bylesjo M, Rantalainen M, Cloarec O, Nicholson J, Holmes E, Trygg J (2006) OPLS discriminant analysis, combining the strengths of PLS-DA and SIMCA classification. J Chemom 20:341–351

Catchpole GS, Beckmann M, Enot DP, Mondhe M, Zywicki B, Taylor J, Hardy N, Smith A, King RD, Kell DB, Fiehn O, Draper J (2005) Hierarchical metabolomics demonstrates substantial compositional similarity between genetically modified and conventional potato crops. Proc Natl Acad Sci USA 102:14458–14462

Chiba Y, Ishikawa M, Kijima F, Tyson RH, Kim J, Yamamoto A, Nambara E, Leustek T, Wallsgrove RM, Naito S (1999) Evidence for autoregulation of cystathionine gamma-synthase mRNA stability in Arabidopsis. Science 286:1371–1374

Fukushima A, Kusano M, Nakamichi N, Kobayashi M, Hayashi N, Sakakibara H, Mizuno T, Saito K (2009a) Impact of clock-associated Arabidopsis pseudo-response regulators in metabolic coordination. Proc Natl Acad Sci USA 106:7251–7256

Fukushima A, Kusano M, Redestig H, Arita M, Saito K (2009b) Integrated omics approaches in plant systems biology. Curr Opin Chem Biol 13:532–538

Goto DB, Naito S (2002) AtMRD1 and AtMRU1, two novel genes with altered mRNA levels in the methionine over-accumulating mto1-1 mutant of *Arabidopsis thaliana*. Plant Cell Physiol 43:923–931

Goto DB, Ogi M, Kijima F, Kumagai T, van Werven F, Onouchi H, Naito S (2002) A single-nucleotide mutation in a gene encoding *S*-adenosylmethionine synthetase is associated with methionine

over-accumulation phenotype in *Arabidopsis thaliana*. Genes Genet Syst 77:89–95

Goto DB, Onouchi H, Naito S (2005) Dynamics of methionine biosynthesis. Plant Biotechnol 22:379–388

Hall RD (2006) Plant metabolomics: from holistic hope, to hype, to hot topic. New Phytol 169:453–468

Hesse H, Hoefgen R (2003) Molecular aspects of methionine biosynthesis. Trends Plant Sci 8:259–262

Hirai MY, Sugiyama K, Sawada Y, Tohge T, Obayashi T, Suzuki A, Araki R, Sakurai N, Suzuki H, Aoki K, Goda H, Nishizawa OI, Shibata D, Saito K (2007) Omics-based identification of Arabidopsis Myb transcription factors regulating aliphatic glucosinolate biosynthesis. Proc Natl Acad Sci USA 104:6478–6483

Inaba K, Fujiwara T, Hayashi H, Chino M, Komeda Y, Naito S (1994) Isolation of an *Arabidopsis thaliana* mutant, mto1, that overaccumulates soluble methionine (temporal and spatial patterns of soluble methionine accumulation). Plant Physiol 104:881–887

Jonsson P, Johansson ES, Wuolikainen A, Lindberg J, Schuppe-Koistinen I, Kusano M, Sjostrom M, Trygg J, Moritz T, Antti H (2006) Predictive metabolite profiling applying hierarchical multivariate curve resolution to GC-MS data—a potential tool for multi-parametric diagnosis. J Proteome Res 5:1407–1414

Jonsson P, Johansson AI, Gullberg J, Trygg J, A J, Grung B, Marklund S, Sjostrom M, Antti H, Moritz T (2005) High-throughput data analysis for detecting and identifying differences between samples in GC/MS-based metabolomic analyses. Anal Chem 77:5635–5642

Kopka J, Schauer N, Krueger S, Birkemeyer C, Usadel B, Bergmuller E, Dormann P, Weckwerth W, Gibon Y, Stitt M, Willmitzer L, Fernie AR, Steinhauser D (2005) GMD@CSB.DB: the Golm Metabolome Database. Bioinformatics 21:1635–1638

Kusano M, Fukushima A, Arita M, Jonsson P, Moritz T, Kobayashi M, Hayashi N, Tohge T, Saito K (2007) Unbiased characterization of genotype-dependent metabolic regulations by metabolomic approach in *Arabidopsis thaliana*. BMC Syst Biol 1:53

Le Gall G, Colquhoun IJ, Davis AL, Collins GJ, Verhoeyen ME (2003) Metabolite profiling of tomato (*Lycopersicon esculentum*) using 1H NMR spectroscopy as a tool to detect potential unintended effects following a genetic modification. J Agric Food Chem 51:2447–2456

Levandi T, Leon C, Kaljurand M, Garcia-Canas V, Cifuentes A (2008) Capillary electrophoresis time-of-flight mass spectrometry for comparative metabolomics of transgenic versus conventional maize. Anal Chem 80:6329–6335

Mootha VK, Lindgren CM, Eriksson KF, Subramanian A, Sihag S, Lehar J, Puigserver P, Carlsson E, Ridderstrale M, Laurila E, Houstis N, Daly MJ, Patterson N, Mesirov JP, Golub TR, Tamayo P, Spiegelman B, Lander ES, Hirschhorn JN, Altshuler D, Groop LC (2003) PGC-1alpha-responsive genes involved in oxidative phosphorylation are coordinately downregulated in human diabetes. Nat Genet 34:267–273

Okazaki Y, Shimojima M, Sawada Y, Toyooka K, Narisawa T, Mochida K, Tanaka H, Matsuda F, Hirai A, Hirai MY, Ohta H, Saito K (2009) A chloroplastic UDP-glucose pyrophosphorylase from Arabidopsis is the committed enzyme for the first step of sulfolipid biosynthesis. Plant Cell 21:892–909

Oksman-Caldentey KM, Saito K (2005) Integrating genomics and metabolomics for engineering plant metabolic pathways. Curr Opin Biotechnol 16:174–179

Onouchi H, Nagami Y, Haraguchi Y, Nakamoto M, Nishimura Y, Sakurai R, Nagao N, Kawasaki D, Kadokura Y, Naito S (2005) Nascent peptide-mediated translation elongation arrest coupled with mRNA degradation in the CGS1 gene of Arabidopsis. Genes Dev 19:1799–1810

Redestig H, Fukushima A, Stenlund H, Moritz T, Arita M, Saito K, Kusano M (2009) Compensation for systematic cross-contribution improves normalization of mass spectrometry based metabolomics data. Anal Chem 81:7974–7980

Rinder J, Casazza AP, Hoefgen R, Hesse H (2008) Regulation of aspartate-derived amino acid homeostasis in potato plants (*Solanum tuberosum* L.) by expression of *E. coli* homoserine kinase. Amino Acids 34:213–222

Schauer N, Steinhauser D, Strelkov S, Schomburg D, Allison G, Moritz T, Lundgren K, Roessner-Tunali U, Forbes MG, Willmitzer L, Fernie AR, Kopka J (2005) GC-MS libraries for the rapid identification of metabolites in complex biological samples. FEBS Lett 579:1332–1337

Shen B, Li C, Tarczynski MC (2002) High free-methionine and decreased lignin content result from a mutation in the Arabidopsis *S*-adenosyl-L-methionine synthetase 3 gene. Plant J 29:371–380

Suzuki A, Shirata Y, Ishida H, Chiba Y, Onouchi H, Naito S (2001) The first exon coding region of cystathionine gamma-synthase gene is necessary and sufficient for downregulation of its own mRNA accumulation in transgenic *Arabidopsis thaliana*. Plant Cell Physiol 42:1174–1180

Thimm O, Blasing O, Gibon Y, Nagel A, Meyer S, Kruger P, Selbig J, Muller LA, Rhee SY, Stitt M (2004) MAPMAN: a user-driven tool to display genomics data sets onto diagrams of metabolic pathways and other biological processes. Plant J 37:914–939

Trygg J, Holmes E, Lundstedt T (2007) Chemometrics in metabonomics. J Proteome Res 6:469–479

Weckwerth W, Loureiro ME, Wenzel K, Fiehn O (2004) Differential metabolic networks unravel the effects of silent plant phenotypes. Proc Natl Acad Sci USA 101:7809–7814

Wu G (2009) Amino acids: metabolism, functions, and nutrition. Amino Acids 37:1–17

Yonekura-Sakakibara K, Tohge T, Matsuda F, Nakabayashi R, Takayama H, Niida R, Watanabe-Takahashi A, Inoue E, Saito K (2008) Comprehensive flavonol profiling and transcriptome coexpression analysis leading to decoding gene-metabolite correlations in Arabidopsis. Plant Cell 20:2160–2176

Zhang P, Foerster H, Tissier CP, Mueller L, Paley S, Karp PD, Rhee SY (2005) MetaCyc and AraCyc. Metabolic pathway databases for plant research. Plant Physiol 138:27–37